Distribution Grid Reliability versus Regulation Market Efficiency: An Analysis based on Micro-PMU Data

Alireza Shahsavari, *Student Member, IEEE*, Ashkan Sadeghi-Mobarakeh, *Student Member, IEEE*, Emma Stewart, Ed Cortez, Lilliana Alvarez, Fady Megala, and Hamed Mohsenian-Rad, *Senior Member, IEEE*

***Abstract*—There is a growing interest among power system operators to encourage load resources to offer frequency regulation. Prior studies have evaluated the system-wide benefits of such load resource participation. However, the potential adverse impact of wide scale load resource participation on distribution system performance, in the *transient* time frame, is often overlooked. Our goal is to address this open problem. We focus on a scenario where load resources offer *regulation down* service. To obtain realistic results, a distribution feeder in Riverside, CA is considered, where distribution-level phasor measurement units are used to collect high resolution voltage and current data. We start by developing a novel *data-driven* approach to analyze *transient* load behaviors. Subsequently, we model the aggregate load transient profile, in form of a three-phase surge current profile, that could be induced on a distribution feeder once a group of loads responds to a regulation down event. The impact of delay, e.g., due to sensing, communications, and load response, is considered. Distribution grid reliability is analyzed by taking into account the characteristics of the main feeder's protection system as well as each lateral's protection system. Both *momentary* and *permanent* reliability indexes are calculated. Case studies suggest that it is possible to jeopardize distribution grid reliability if several regulation down load resources are on the same feeder. Depending on various factors with respect to load resources, distribution feeder, and regulation market, there may or may not exist ways to break the *trade-off* between distribution grid reliability and regulation market efficiency. The construction and analysis of the *reliability-efficiency curves* would be needed for each feeder.**

***Keywords*: Load resources, micro-PMUs, data-driven analysis, distribution grid reliability, regulation down service efficiency.**

NOMENCLATURE

t_{op}, t_{trip}	Operation time and tripping time
t_s, t_r	Switching time and repairing time
I, I_P	Input current and peak-up current
θ, θ_{max}	Disk travel and maximum disk travel
τ	Delay time: sensing, communications, etc.
K, α	Constant relay parameters
Φ	Set of annual line contingencies
Γ	Set of annual transformers contingencies
Ψ	Set of annual regulation down contingencies
$\lambda^{p/m}$	Permanent/momentary interruption frequency
n	Number of interrupted customers
r	Interruption duration
N	Total number of customers
ρ	Probability of regulation service contingency
T	Equilibrium temperature of fuse
m, c	Equilibrium mass and thermal capacity of fuse
K_f	Thermal conductivity coefficient of fuse
R_f	Resistance of fuse at $25\,^{\circ}\mathrm{C}$
α_f	Resistance temperature coefficient

A. Shahsavari, A. Sadeghi-Mobarakeh, and H. Mohsenian-Rad are with the Department of Electrical and Computer Engineering, University of California, Riverside, CA, USA, e-mail: {ashah023,asade004}@ucr.edu and hamed@ece.ucr.edu. E. Stewart is with the Lawrence Livermore National Laboratory, Livermore, CA, USA, e-mail: stewart78@llnl.gov. E. Cortez, L. Alvarez, and F. Megala are with Riverside Public Utilities, Riverside, CA, USA, email:{ecortez, lalvarez, fmegala}@riversideca.gov. This work was supported by RPU grant 14-2853, NSF grants 1253516, 1307756, 1462530, and DoE grant EE 0008001. The corresponding author is H. Mohsenian-Rad.

I. INTRODUCTION

System frequency in power systems is maintained with a careful balance of load and generation, mostly by adjusting the output level of generation resources. However, there is now a growing trend in practice to encourage offering frequency regulation also by controllable loads. Examples of controllable loads that are considered to offer frequency regulation include air-conditioning units [1]–[5] and electric vehicles [6]–[10].

While the system-wide benefits of using load resources for frequency regulation are studied well, e.g., see [1], [11]–[14], the current literature often overlooks the potential impact on power distribution feeders, due to the lack of available monitoring and accurate distribution system models. Note that, based on the hierarchical structure of the power grid, any system-wide service that is offered by load resources is physically mediated by distribution feeders. Therefore, it is of critical to examine whether and to what extent the use of load resources could have an adverse effect on the operation of distribution systems. To the best of our knowledge this problem is not addressed yet.

Addressing the above open problem is the focus of this paper. Specifically, we consider the regulation *down* service, which requires decreasing generation or increasing consumption when frequency exceeds a threshold [15]. To obtain realistic results, a real-world distribution feeder is considered in Riverside, CA, where distribution-level phasor measurements units, i.e., μPMUs, are used to collect *high resolution, time synchronized* voltage and current data at 120 readings per second. The contributions in this paper can be summarized as follows:

1) A novel *data-driven* approach is developed to use experimental μPMU data, on three phases, to analyze *transient* behaviors of different regulation down load resources.
2) A new method is developed to model the aggregate load transient profile, in form of an aggregate surge current profile, that is induced on a distribution feeder once a group of load resources responds to a regulation down event. This is done by applying pattern recognition methods, and taking into account factors such as sensing delay, communications delay, and load response delay,
3) A comprehensive distribution grid reliability analysis is conducted for the under-study distribution system, in

presence of regulation down load resources, by taking into account the models and different characteristics of the main feeder's protection system as well as each lateral's protection system. Based on whether or not a recloser device is used in the protection system, both *momentary* and *permanent* reliability indexes are analyzed.

4) The above reliability analysis is combined with an analysis on performance score calculation in performance-based regulation markets. Accordingly, a methodology is derived to investigate the potential *trade-off* between distribution grid reliability and regulation market efficiency.
5) It is shown that the surge current induced by regulation down load resources can have severe adverse effect on the protection system, and thus on the reliability of distribution networks. One may attempt to mitigate such adverse effect by adding sufficiently large and randomly selected intentional delays to the response time of the regulation down load resources. However, this has to be done carefully, because while *reshaping* the load resources' aggregate surge current may help to avoid jeopardizing reliability, it should *not* be to the extent that it jeopardizes their performance in offering regulation down service. In practice, there may or may not exist a *safe choice* for the amount of added random delays to break the trade-off. The careful construction and analysis of the reliability-efficiency curves would be critical.

Besides the literature on load-assisted frequency regulation, this paper is also related to the broad literature on distribution system reliability. While the majority of studies in this field addressed contingencies that are triggered by *non-electric* causes, such as a downed power line [16]–[18] our analysis is more comparable to the smaller group of papers, e.g., in [19, pp. 40-45], that addressed contingencies that are triggered by electric causes. In our case, the contingency is due to the aggregate surge current induced by a regulation down event.

II. Regulation down Service and Load Resources

Frequency regulation is the mechanism of balancing power generation and power consumption in real time to maintain the stability and reliability of the power system. If generation is less than consumption, then frequency drops and *regulation up* service is needed. If generation is greater than demand, then frequency increases and *regulation down* service is needed.

The focus in this paper is on regulation down service, which is needed during regulation down events. A *regulation down event* occurs when the frequency exceeds its nominal value, e.g., 60 Hz in the U.S. Regulation down service is provided by a generator, when it decreases its generation, or by a load resource, often through an aggregator, when it increases its consumption during the requested time frame [5].

It is worth pointing out that the impact of regulation up service is not considered in this study. Offering regulation up service at distribution level may potentially cause issues with power quality. However, it often does not involve surge currents and it is unlikely to raise any major reliability issue.

Many independent system operators (ISOs) have recently adopted mechanisms to allow load resources to offer regulation services. For example, the California ISO (CAISO) has a program for Non-Generator Resources (NGRs) with Regulation Energy Management (REM) to enable resources with limited energy capacities to competitively bid in the regulation market [5]. The PJM inter-connection has also introduced the RegD and RegA regulation signals to encourage fast responding loads, generators, and storage units to provide regulation services [7].

Both CAISO and PJM run *performance-based* regulation markets, where the payments to regulation resources are calculated based on how fast and accurately they respond to regulation signals. Specifically, the payments to regulation resources are adjusted based on their *performance accuracy score*, a.k.a., energy precision score, which is a number between 0 and 1. A higher score indicates better regulation performance and leads to a higher payment. If the performance accuracy score of a regulation resource drops below a certain threshold, e.g., 0.5 in the CAISO regulation market, then the resource is ultimately *disqualified* to provide regulation services [15].

We denote the performance score as PS. It is calculated once for each market interval. Mathematically, we can write [14]:

$$\mathrm{PS} = \left[1 - \frac{\sum_{\sigma=1}^{T} |\ s[\sigma] - y[\sigma]\ |}{\sum_{\sigma=1}^{T} s[\sigma]} \right]^{+}, \tag{1}$$

where $s[\sigma]$ denotes the regulation set point at each performance accuracy evaluation time slot σ and $y[\sigma]$ denotes the mechanical output of the regulation resource at that time slot. The length of the time slots may vary depending on the ISO market. For example, CAISO examines performance accuracy once every four seconds [20]. PJM examines performance accuracy once every two seconds for fast resources and once every ten seconds for slow resources [21]. Note that, $[x]^+ = \max\{0, x\}$ and T is the total number of time slots within the market interval. The fraction in (1) is a normalized measure of performance *inaccuracy* in following the regulation set points, where $|\,s[\sigma] - y[\sigma]\,|$ is the *error* in following the regulation set point.

Note that, the focus in this paper is *not* on determining or coordinating the frequency regulation threshold parameters for load resources. Instead, the focus is on the moment (and a few seconds after) when a frequency event is triggered, with a preset threshold parameter. In other words, what happens *after* such event is triggered, with the load resources and consequently also with the distribution feeders, is of our concern in this paper.

III. Data-Driven Load Transient Models

The impact of flexible load resources providing regulation down service on distribution system reliability can be studied under both *steady-state* and *transient* frameworks. In the steady-sate, the load resources must satisfy *load flow* constraints. This is addressed, e.g., in [22]. What is less understood is the potential adverse impact on power distribution transients, and consequently network reliability. To address this open problem, one shall investigate the transient behavior of load resources at the moment that they are called upon, i.e., when a regulation down event occurs. One option is to derive a mathematical dynamic model for each load. This would require accurate knowledge about all loads, which is difficult because these resources are owned and operated by customers. With hundreds of feeders serving hundreds of thousands of customers, the human and computational resources that are needed to build the modeling framework to represent every load would significantly outwith that of the average utility. Alternatively, in this section, we develop a *data-driven* model for load transients using data from distribution-level phasor measurement units.

A. Individual Load Transient Signatures

Distribution-level phasor measurement units, a.k.a., μPMUs, are new power system sensors that are deployed on distribution feeders to provide precise GPS-synchronized reading of voltage and current phasors to support various applications [23]–[28]. In this paper, we use the experimental data from two μPMUs that are installed at the secondary side of two pad-mounted 12.47 kV to 480 V transformers in Riverside, CA. The sampling rate is 120 Hz, i.e., one sample every 8.333 msec. This high sampling rate, and the fact that we have access to voltage and current data and not just power data, allow us capture the load transient within a data-driven framework.

Four fundamental measurements on three phases are derived from each μPMU: voltage magnitude, voltage phase angle, current magnitude, and current phase angle. In this paper, we use the *current magnitude* to understand the dynamics of the current surge when a major load device, such as an air-conditioner, is hypothetically called upon at a regulation down event. This is because, as we will explain in Section IV, most practical distribution protection relays and fuses are sensitive to spikes in the current magnitude.

The central idea in our data-driven load transient modeling approach is to examine the current magnitude data during one week, July, 1 to July 7, 2016, to identify and analyze all major *current surge signatures*. To such aim, we examined the maximum magnitude of the current synchrophasors during each spike event, and compared it with the average magnitude across a time window of raw synchrophasor data, before and after the spike. If the ratio was above a certain threshold, across all three phases, then the spike signature would be captured.

In total, we analyzed $120 \times 60 \times 60 \times 24 \times 3 \times 7 = 217,728,000$ current magnitude readings per μPMU. Accordingly, we identified 1,803 current surge signatures with at least 40% momentary spikes in the current magnitude across all three phases. Each current spike takes from only a few milliseconds to a several hundred milliseconds. A closer look at the collected data revealed that these signatures can be clustered into a few groups with similar-shaped signatures in each group. Clustering was done using the *fuzzy C-means clustering method* from pattern recognition, c.f. [29], where C indicates the number of clusters, fixed apriori based on the following features:

- Peak to mean magnitude value;
- Start to peak time, i.e., rise time;
- Start to end time, i.e., Settling time.

The clustering problem is solved by considering five clusters, which resulted in 99.13% average dependency to centres, which indicates that the signatures in each cluster are indeed repetitions or slight variations of each other. Thus, we identified *five load clusters*, that are responsible for the majority of the current surges seen by the μPMUs. They are shown in Fig. 1. All five signatures are believed to belong to building Heating Ventilation and Air-Conditioning (HVAC) loads. Accordingly, their corresponding five load units are proper candidates to be recruited as frequency regulation load resources, see [5].

B. Aggregate Load Transient Profiles

Suppose there are N regulation down load resources of M different load types across a distribution feeder. In a typical distribution feeder in today's power systems, where the penetration of distributed generation resources is still relatively small, the instantaneous current that goes through the protection relay at the feeder head is the summation of the instantaneous current that is drawn by each load. Therefore, we can use the setup in Fig. 2 to calculate the transient current that goes through the feeder's protection system at and a few moments after a regulation down event occurs. In this figure, without loss of generality, we assume that $N > 5$ and the load resources are of the $M = 5$ types in Fig. 1. The transformers are considered to be ideal and linear with turns-ratio $TR = n_P/n_S$.

For the model in Fig. 2, the aggregate current load profile is decomposed into two components. The first component is the *feeder background load* that is the summation of the current that is drawn by all loads that do *not* offer regulation down service. At the millisecond time resolution in our analysis, the feeder background load is considered as a constant at and around the moment that a regulation down event occurs. The second component is an *aggregate current profile* of the N loads that *do* offer regulation down service. This second component is the one that generates the transient response at and around the moment that a regulation down event occurs. Here, we are essentially modelling the loads at and around the moment that a regulation down event occurs as constant current, c.f. [30].

In practice, there is often a slight *lagging*, i.e., a small delay (typically bounded by 2 or 4 seconds due to regulation market requirements), between the moment that the regulation down event occurs and the moment that the current surge signature appears for each regulation down frequency responsive load. For each load unit $i = 1, \ldots, N$ such delay is modelled as:

$$\begin{aligned} \text{Delay } \tau_i = \; & \text{Sensing Delay +} \\ & \text{Communications Delay +} \\ & \text{Load Response Delay.} \end{aligned} \tag{2}$$

If frequency is sensed locally by each load, then communications delay is not a factor, but the sensing delay is a factor as it is often different at different loads. If regulation down commands are dispatched by a central entity, then communications delay has significant impact. Regardless of the method of sensing/communicating, load response delay could be different for different loads based on their internal control mechanisms. Note that, the load response delay may include an *intentional* delay component, as we will discuss below and in Section V.

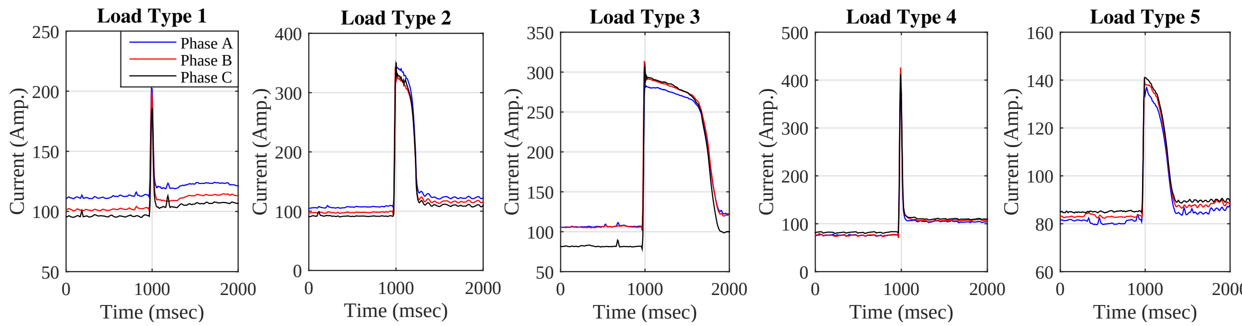

Fig. 1. The five *current surge signatures* that represent the five load types with significant current surges that are identified through analysis of μPMUs data.

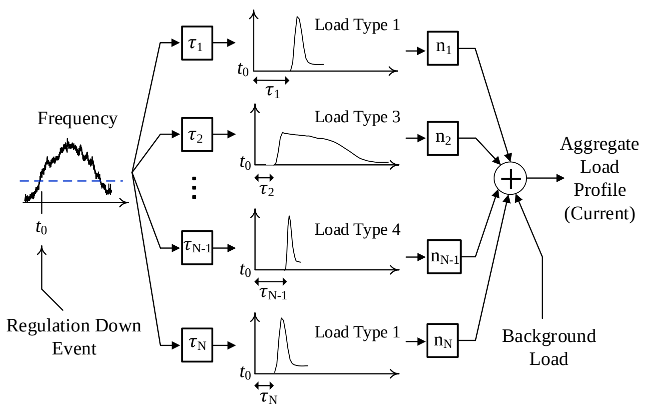

Fig. 2. The method of calculating the aggregate load current profile at a regulation down event under different load types and different delay values.

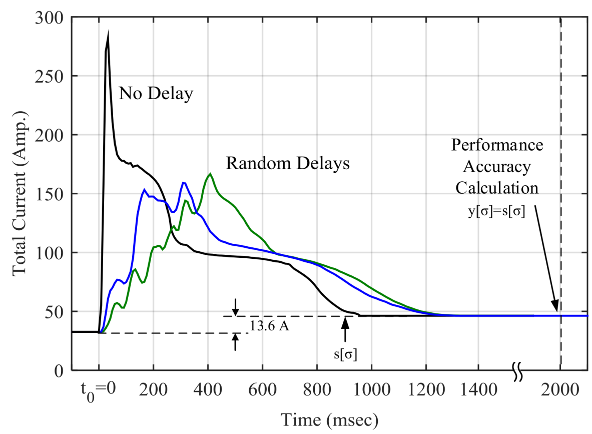

Fig. 3. Examples of the aggregate load transient profile under different delay scenarios. The regulation down event is assumed to occur at time zero.

To gain insight on the role of delay, suppose 30% of the loads at downstream of the under-study 12.47 kV to 480 V transformer, are a mix of $M = 5$ load types that offer regulation service. If $\tau_1 = \ldots = \tau_N = 0$, i.e., there is absolutely no delay, then the single phase aggregate load transient profile is obtained with a large spike, as marked in Fig. 3. Of course, in practice, there are always *some* delays, as noted in (2). Therefore, this figure also shows two different realizations where the delays are random with a discrete uniform distribution up to 400 msec. We can see that random delays can result in different aggregate load transient profiles. In particular, they naturally help reducing the size of the spike in the aggregate current signature. However, if the delay is, possibly intentionally, too large, then it can affect performance accuracy, creating a *trade-off* between distribution grid reliability and regulation market efficiency. We will further evaluate and characterize such trade-off in the rest of this paper.

IV. Analysis of Distribution Grid Reliability

A. Feeder Main Protection System Model

The most common relays at distribution level are electromechanical over-current, equipped *with* or *without* reclosing capability [31]. The over-current relay operates, i.e., picks up, when the feeder current exceeds a threshold, a.k.a., the *pick-up current*. The over-current relays are categorized based upon their time-current characteristics (TCC). The relays in the under-study feeder are the inverse definite minimum time (IDMT) relays, which are commonly used by most utilities [32].

In electromechanical IDMT relays, which are of interest in this paper, the TCC inversely depends on the current. The TCC in pick-up/reset modes can be derived from the dynamic equation of the relay's induction disk rotation with respect to contingency current, see [32]. The tripping criteria becomes:

$$\int (1/t_{op})dt = 1. \tag{3}$$

where, t_{op} is calculated by considering time multiplier setting (TMS) as well as by imposing intentional delay time as:

$$t_{op} = TMS\left(\frac{K_{op}}{(I/I_P)^{\alpha_{op}} - 1} + L\right). \tag{4}$$

Here, I denotes the total current that goes through the relay in a time frame that starts at the moment when a regulation down event occurs, i.e., time t_0, and ends once the current reaches its steady-state, with curves similar to those in Fig. 3.

Similar to tripping, the reset time for $I \leq I_P$, while reset time multiplier setting (RTMS) is imposed:

$$t_{reset} = RTMS\left(\frac{K_{reset}}{1 - (I/I_P)^{\alpha_{reset}}}\right). \tag{5}$$

The constant coefficients K_{op} and K_{reset} depend on the relay type and the standard being used. The TCC coefficients of tripping and resetting for the common relays are given in [33].

In our analysis, we also consider the case where the feeder protection system is reinforced by an instantaneous over-current element, which operates with no intentional delay.

B. Lateral Protection System Model

The lateral branches in this study are equipped with cut-out fuses, where a fusible element made of tin or silver melts under current surges and overloads. Thus, the melting period lasts from sensing an over-current to when the fuse link melts. The melting dead-time of each fuse depends on the magnitude and the duration of surge current, which is presented in TCC as minimum melt curve and the maximum total clear curve.

The melting time of a fuse-link can be calculated using either joule-integral equations [34] or heat transfer equations [35]. However, most existing models need inaccessible data of fuses in practice and rarely provide a straightforward dynamic model for intermittent heating and cooling periods. Therefore, in this paper, we reformulate the thermal heat transfer model and address to include the dynamic equation for heating period, when I exceeds the minimum melting current corresponding to TCC, with respect to the contingency current:

$$\dot{T} = \frac{1}{m \cdot c} \left(R_f \left(1 + \alpha_f T\right) I^2 - K_f \left(T - T_a\right)\right), \qquad (6)$$

where $T(0) = T_a$. Suppose the solution of the above differential equation is $T(t) = f(I, \alpha_f, T_a, R_f, m, c, K_f)$. In theory, I is the only input into this solution; the rest of parameters are supposed to be known. However, in practice, m, c, and K are not provided by the manufacturer. Therefore, in this paper, we consider n arbitrary points I_i and t_i from the TCC of each fuse and set $T(t_i) = T_m$. We then solve a system of n non-linear equations to obtain all unknown parameters. This is done using exhaustive search. The known parameters are set based on the S&C 100 A QR speed fuse: $T_m = 800\,°\mathrm{C}$, $R_f = 1\Omega$, and $\alpha_f = 0.0001\Omega/°\mathrm{C}$ [35], which results $mc = 162.91$ and $K_f = 47.18$. The impact of pre-loading and ambient temperature on melting time are considered based on [36]. The dynamic model during cooling period is derived from [37].

C. Reliability Evaluation Under Regulation Down Service

We are now ready to evaluate how the distribution grid reliability is affected due to recruiting and integrating load resources into the regulation down market. We use the following three models that we developed earlier: the aggregate current profiles under regulation down events from Section III-B; the relay response models from Section IV-A; and the fuse response models from Section IV-B. We will investigate whether and how the feeder's main and lateral protection systems, and consequently the distribution grid reliability, are affected in presence of distributed regulation down load resources.

The impacts on network reliability depend on the protective device settings and the magnitude and surviving time of surge current. For instance, the customers located at the downstream of a lateral experience an interruption, if the aggregated surge current at lateral exceeds the minimum melting current of fuse as well as survives enough in heating period to melt the fuse link. Also, it is possible that the aggregated surge current exceeds its predetermined pick-up current of the relay at the main feeder and stay long enough to trip the relay. Accordingly, *full* or *zonal* interruptions may occur across the feeder.

The impact of such service interruptions can be analyzed using the prevalent reliability indexes: System Average Interruption Duration Index (SAIDI), System Average Interruption Frequency Index (SAIFI), and Average Energy Not Supplied (AENS) [16], [38]. For the purpose of the study in this paper, the standard calculation of these indexes are adjusted as follows:

$$\text{SAIFI} = \frac{1}{N} \times \left(\sum_{i \in \{\Phi \cup \Gamma\}} \lambda_i^p n_i + \sum_{i \in \Psi} \rho_i n_i \right), \qquad (7)$$

$$\text{SAIDI} = \frac{1}{N} \times \left(\sum_{i \in \{\Phi \cup \Gamma\}} \lambda_i^p r_i n_i + \sum_{i \in \Psi} \rho_i r_i n_i \right), \qquad (8)$$

$$\text{AENS} = \frac{1}{N} \times \left(\sum_{i \in \{\Phi \cup \Gamma\}} \lambda_i^p r_i P_i + \sum_{i \in \Psi} \rho_i r_i P_i \right). \qquad (9)$$

The first term inside the parenthesis in each case indicates the interruption frequency/duration due to typical fault occurrences in the main feeder and in the laterals, that are *not* related to the market participation of load resources. The second term, however, indicates the imposed interruption frequency/duration due to the surge current caused by the switch on events of the regulation down market participating load resources.

If the main protection system is reinforced by a recloser, see Section V-B, then we shall investigate the *momentary* reliability indexes [39], such as the Momentary Average Interruption Frequency Index (MAIFI), where the recloser and lateral fuses are coordinated, see [40], [41]. Again, for the purpose of this paper, the standard calculation of MAIFI is adjusted as follows:

$$\text{MAIFI} = \frac{1}{N} \times \left(\sum_{i \in \{\Phi \cup \Gamma\}} \lambda_i^m n_i + \sum_{i \in \Psi} \rho_i n_i \right). \qquad (10)$$

While the first terms in (7)-(10) can be set based on the utility's reliability documents and historical data, e.g., see [38], the second terms in (7)-(10) are currently unknown in the literature and the power engineering community. However, in this paper, and as we will see in the next section, we use experimental data and the methodologies described in Sections V-A and V-B to calculate these additional reliability terms.

V. Case Studies

The single-line diagram of the under-study 12.47 kV three-phase feeder in Riverside, CA is shown in Fig. 4. It is assumed to serve 10 MVA load, mostly commercial. The main feeder is 4.3 miles long, that is carved up into 10 zones based on its available protective and control devices as listed in Table I. The main feeder is protected by over-current electromechanical phase relays with instantaneous unit connected to a three-phase circuit breaker. The phase over-current relays work in extremely inverse mode with operation parameters $K_{op} = 28.2$, $\alpha_{op} = 2$, $L = 0.1217$ and reseting parameters $K_r = 29.1$ and $\alpha_r = 2$ [33]. The time dial setting tap and the pick-up current setting tap are set to one and eight, respectively. The instantaneous pick-up current setting tap is set to 25. Most laterals are

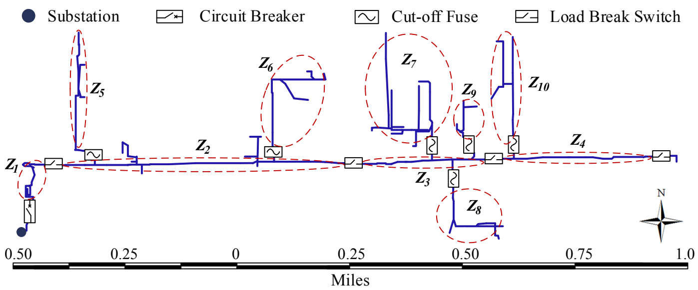

Fig. 4. The single-line diagram of the under-study feeder in Riverside, CA.

TABLE I
THE CHARACTERISTICS AND PARAMETERS OF EACH ZONE.

Zone	Number of Customers	Length (Mile)	Number of Transformers	Load (kVA)
Z_1	0	0.12	0	0
Z_2	30	0.62	3	750
Z_3	20	0.30	2	500
Z_4	20	0.32	1	500
Z_5	30	0.35	3	750
Z_6	60	0.33	5	1,500
Z_7	90	1.05	5	2,250
Z_8	60	0.45	2	1,500
Z_9	40	0.12	3	1,000
Z_{10}	50	0.64	3	1,250
Total	400	4.30	27	10,000

protected by fuses as shown in Fig. 4. For instance, the lateral marked as Z_8, which serves two 750 kVA transformers, is protected by an S&C 100 A QR speed fuse. The real-life under-study feeder is not reinforced by a recloser; nevertheless, we do study the impact of a recloser on the overall reliability indexes.

Unless stated otherwise, we assume that the regulation down load resources are called once a day. The default probability of annual permanent and annual momentary failures on lines are set to 0.065 and 0.06 faults per km, respectively [38]. The annual permanent and annual momentary failure rates of transformers are set to 0.015 and 0.050 [38]. Based on the length of the under-study feeder, the restoration time for both tripped relay and blown fuse will be 30 minutes, while the average switching period is one hour. Line repair time is assumed to be three hours [38]. Given the often long repair time for a faulted transformer, it is typical to set the repairing time to be equal to the replacement time, i.e., five hours.

The distribution of the load types across the transformers was random, but it followed the same ratio at which the transient signatures appeared in the signature database. Those ratios are 6.99%, 7.41%, 42.98%, 20.03%, and 22.38%, for load type 1 to 5, respectively. For example, we assumed that each transformer may on average experience 6.99% of its surge current during a regulation down event from load resources of type one.

A uniform delay distribution is considered for each load resource, which represents the sensing delay, the communication delay, and the response delay, see (2). Even though the response delays are similar within each load type, the two former delays are different for each individual resource.

TABLE II
LOAD POINT RELIABILITY EVALUATION UNDER NATURAL PERMANENT CONTINGENCIES FOR THE LOADS THAT ARE LOCATED IN ZONE Z_8.

Faulted Zone	λ^p (f/hr)		r (hr/f)	U (hr/yr)	ENS (kWh/yr)
	Line	Trans.			
Z_1	0.0125	0	t_s	0.0125	18.8292
Z_2	0.0648	0.045	t_s	0.1098	164.784
Z_3	0.0313	0.030	t_r	0.2441	366.219
Z_4	0.0334	0.015	t_s	0.0484	72.7114
Z_5	0	0	0	0	0
Z_6	0	0	0	0	0
Z_7	0	0	0	0	0
Z_8	0.0470	0.030	t_r	0.2912	436.829
Z_9	0	0	0	0	0
Z_{10}	0	0	0	0	0
Total	0.3093		2.2830	0.7062	1059.37

A. Impact of Regulation Down Service on Lateral Protection

In this section, we study the dynamic response of the lateral fuses to the surge current caused by regulation down load resources. Load point reliability analysis is done for two cases:

- *Case I:* with no delay in load responses,
- *Case II:* with natural delay in load responses.

For *Case II*, the added natural delay has a uniform distribution between 0 to 1 second, see (1). The number of each signature in aggregated surge current is considered as random to meet about 33% load participation in regulation down service.

Without loss of generality, we focus on zone Z_8, which serves two 750 kVA transformers and is protected by an S&C 100 A QR speed fuse. The analysis is done for 10,000 random scenarios to obtain the probability of fuse blowing and its impact on load point reliability indexes. The results on load point reliability evaluation for the loads located in zone Z_8 under *natural* permanent contingencies, i.e., all permanent contingencies *other than* those caused by regulation down service, are shown in Table II. Note that, a fault occurred in zones Z_5, Z_6, Z_7, Z_9, and Z_{10} has no impact on the load point reliability in zone Z_8. Therefore, all entries in the rows corresponding to these zones are zero. The momentary interruption frequency due to natural momentary faults is 1.7652 f/yr in this case. The probability of fuse melting for *Case I* and *Case II* is 0.0040 and 0.0005, respectively. Accordingly, in *Case I*, customers located in zone Z_8 experience 1.46 permanent contingencies per year due to the presence of regulation down load resources, which last for 0.73 hours per year. While, in *Case II*, the frequency and duration of interruptions that are caused due to regulation down resources will be 0.1825 f/yr and 0.0912 hr/yr, respectively.

The overall momentary and permanent load point reliability indexes for zone Z_8 are shown in Table III. The interruption frequency, i.e., λ, and the interruption duration, i.e., U, increase more in *Case I* than *Case II*, because the natural delay leads to damping surge current over time. Note that, the interruption duration per fault, i.e., r, is less than the base cases for both *Case I* and *Case II*, see the last row in Table II. Therefore, regulation down service with and without delay increases frequency and duration indexes, while the interruption duration per fault reduces due to the imposed short-time interruptions.

TABLE III
LOAD POINT RELIABILITY INDEXES UNDER NATURAL FAULTS AND REGULATION DOWN CONTINGENCIES

Case	λ^m	λ^p	r (hr/f)	U (hr/yr)	ENS (kWh/yr)
I	3.2252	1.7693	0.8117	1.4362	2154.37
II	1.9477	0.4918	1.6214	0.7974	1196.24

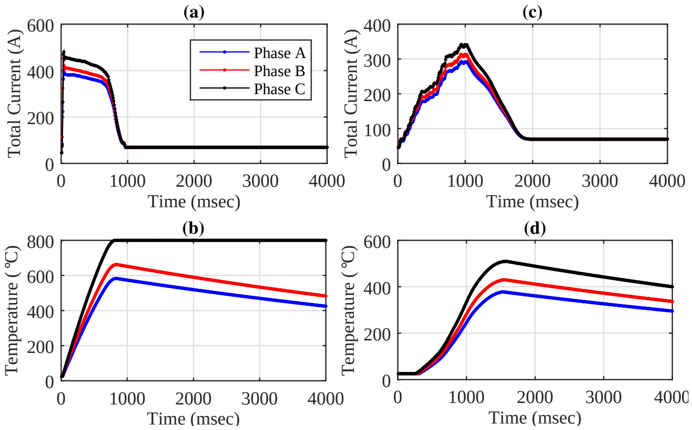

Fig. 5. Dynamic response of fuse, in terms of total current and temperature, to a regulation down surge current: (a) and (b) are for the case *without* added random delay; (c) and (d) are for the case *with* added random delay.

Fig. 5 shows the dynamic responses of fuse to two sample three-phase surge currents induced by regulation down load resources for *Case I* and *Case II*, respectively. In *Case I*, the transient of surge current is 915 msec, while the heating period is from $t = 0$ to $t = 833$ msec. This results in melting the fusible element in *Phase C*. However, in *Case II*, even though the surge current survives more than 1,800 msec and the heating period lasts for 1,250 msec, the magnitude of the surge current is not enough to melt the fuse. Thus, while customers experience outage due to regulation down service contingency in *Case I*, there is no service interruption in *Case II*.

So far, and based on the obtained results, we can conclude that the adverse effect of regulation down surge currents can be mitigated by adding sufficiently large and randomly chosen delays to the response time of regulation down load resources. However, large intentional delays can in turn have adverse effect on the performance of the regulation down service. Therefore, next, we investigate the sensitivity of fuse melting probability to intentional delay. The results are plotted in Fig. 6. As expected, the added intentional delay mitigates the adverse impact on lateral protection by decreasing the probability of fuse melting. Note that, the exact decaying rate in the curve in Fig. 6 depends on the features of the understudy protection system as well as the type, size, and number of load resources.

B. Impact of Regulation Down Service on Main Protection

In this section, we study the dynamic response of the main protection relay to the surge current caused by regulation down load resources. Again, we compare *Case I* and *Case II* as defined in Section V-A. It is assumed that 20-25% of loads participate in regulation down service, while the number of each load type in aggregated surge current is considered as

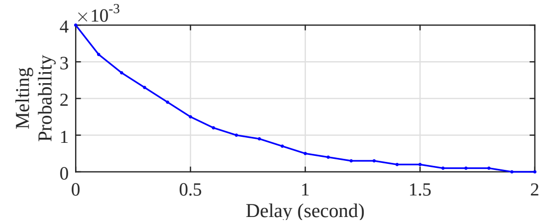

Fig. 6. Fuse melting probability versus the delay in response time of load resources. The fuses are located on laterals.

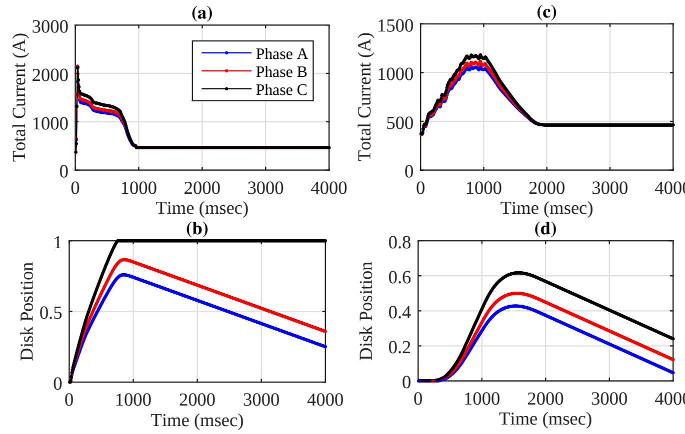

Fig. 7. Dynamic response of relay, in terms of total current and disk position, to a regulation down surge current: (a) and (b) are for the case *without* added random delay; (c) and (d) are for the case *with* added random delay.

random variable. The problem is solved 10,000 times for each case study to obtain probability of relay tripping, followed by reliability evaluation with respect to natural permanent and momentary contingencies. Network reliability indexes due to natural faults are: SAIFI = 0.3277, SAIDI = 0.8219, CAIDI = 2.5081, AENS = 20.5484, ASAI = 0.999906, and MAIFI = 1.7652. For each random scenario, the analysis is done for four different setups: *with* and *without* recloser as well as *with* and *without* instantaneous relay element. Recall that, if the feeder is reinforced by recloser, then the current surge that is induced by regulation down load resources may affect only the momentary reliability indexes, not the permanent reliability indexes.

The obtained results are presented in Table IV, including the tripping probabilities of over-current relay, denoted by 51P, instantaneous element, denoted by 50P, as well as both over-current relay and instantaneous element, denoted by 50P & 51P. Although the tripping probabilities under contingencies are calculated per phase, the reported values are probability of circuit-breaker tripping since as mentioned before, the feeder is reinforced by a three-phase breaker. We can see that, for *Case I*, where there is no delay, the instantaneous element is more sensitive to the surge current than the over-current relay. This means that the main challenge with regulation down surge current is the magnitude rather than the transient period. In *Case II*, where there is some natural delay, the surge currents of different load resources are spread out in time; hence, the aggregate surge current often, i.e., in 97% of the random scenarios, does *not* exceed the setting of the instantaneous element. Of course, it takes longer for the aggregate surge current to settle down in this case.

TABLE IV
DIFFERENT RELAY CASES AND THEIR CORRESPONDING RELIABILITY RESULTS UNDER REGULATION DOWN CONTINGENCIES

Case	Tripping Probability			Without 50P				With 50P			
				Without Recloser			With Recloser	Without Recloser			With Recloser
	51P	50P	50P & 51P	SAIFI	SAIDI	AENS	MAIFI	SAIFI	SAIDI	AENS	MAIFI
I	0.1795	0.7835	0.1720	65.8452	33.5806	839.51	67.2827	286.305	143.810	3595.2	287.742
II	0.0300	0	0	11.2777	6.29693	157.42	12.7152	11.2777	6.29693	157.42	12.7152

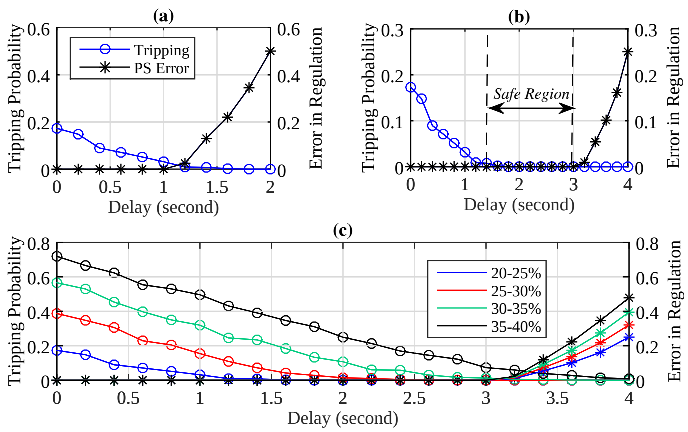

Fig. 8. Tripping probability versus error in regulation service, both in terms of increasing the delay in response time of load resources: (a) Regulation performance is calculated at 2 sec and 20-25% of loads offer regulation down service; (b) Regulation performance is calculated at 4 sec and 20-25% of loads offer regulation down service; (c) Regulation performance is calculated at 2 see and different percentages of loads offer regulation down service.

We can see in Table IV that adding delays results in significant reduction in permanent and momentary reliability indexes, with respect to frequency, duration, and energy.

Figs. 7 shows the dynamic responses of the over-current relay to two sample three-phase surge currents induced by regulation down load resources for *Case I* and *Case II*, respectively. Similar results could be obtained for the instantaneous element relay. From Fig. 7(a), the transient of surge current is almost 1000 msec, while the tripping period last for about 700 msec. Accordingly, the surge current corresponding to *phase C* satisfies (3), while in the rest of phases the disk rotates in the resetting direction before travelling one cycle. However, in Fig. 7(c), though the surge current survives more than 1800 msec and the tripping period lasts for almost 1100 msec, the magnitude of surge current is not large enough to satisfy 3, see the slope of the tripping period in Fig. 7(b) and (d).

C. Reliability-Performance Tradeoff

So far, and based on the results that we obtained in Sections V-A and V-B, we can make two main conclusions:

1) The surge current induced by regulation down load resources can have severe adverse effect on the protection system, and thus the reliability of distribution networks.
2) One can mitigate such adverse effect by adding sufficiently large and randomly chosen intentional delays to the response time of the regulation down load resources.

While the second item above is good news, it immediately raises the concern on whether adding intentional delays can have adverse effect on the performance of the regulation down service. Note that, if this "solution" ends up jeopardizing regulation down performance then it *defeats the purpose* of offering regulation down service by load resources.

The key to understand and characterize the above trade-off is to reexamine the results in Fig. 3 in Section III-B. Accordingly, one may now ask the following two fundamental questions:

1) How much random delay shall we add to the response time of load resources such that, while we *reshape* their aggregate surge current to avoid jeopardizing reliability, we also do *not* postpone their settling down time to the extent that it jeopardizes their regulation down service?
2) Does there always exist a *safe choice* for the amount of the added random intentional delays in order to satisfy the requirements in the first question above?

One can answer the above questions using the curves in Fig. 8, where we plot the tripping probability and the error in regulation service. The latter is defined in Section II. Both curves are plotted versus the delay in the response time of load resources. First, consider Fig. 8(a), where performance accuracy is calculated once every two seconds, as in the case of fast resources in PJM. Here, any choice of delay would inevitably degrade either reliability or efficiency. Next, consider Fig. 8(b), where performance accuracy is calculated once every four seconds, as in CAISO. Here, there is a *safe region* for the choice of delays, without degrading reliability or efficiency.

The curves in Fig. 8 depend on the features of the under-study feeder as well as the type, size, and number of load resources. For example, while the current 20-25% load participation rate in Fig. 8(b) is manageable as long as the delays are set properly, increasing the participation rate can reduce or even eliminate the *safe region*, as shown in Fig. 8(c).

Ultimately, one needs to obtain the curves such as those in Fig. 8(c) for every feeder with large amount of load resources before trying to integrate those load resources into regulation market. One will have to properly limit the participation rate in each feeder, because above a certain level even a carefully selected delay mechanism cannot break the tradeoff between distribution grid reliability and regulation market efficiency.

VI. CONCLUSIONS

This paper takes the first steps in analyzing the reliability of power distribution systems in presence of regulation down load resources. Using the parameters of a distribution feeder in Riverside, CA, together with experimental μPMU data from the same distribution feeder, and also by taking into account the current surge signatures of practical regulation-eligible load types, the characteristics of practical distribution-level protection devices, both on the main feeder and its laterals, and the impact of delay, e.g., due to sensing, communications, and load response, we showed that it is possible to jeopardize distribution grid reliability if several regulation down load resources are on the same feeder. Moreover, we developed a data-driven method to evaluate the trade-off between distribution grid reliability and regulation market efficiency. We showed under what conditions one may or may not break such trade-off by adding properly setup intentional random delays to the response time of the regulation down load resources. The results in this paper could be of value to utilities, aggregators, and system operators.

References

[1] H. Hao, B. Sanandaji, K. Poolla, and T. Vincent, "Potentials and economics of residential thermal loads providing regulation reserve," *Energy Policy*, vol. 79, pp. 115–126, 2015.

[2] O. Erdinç, A. Taşcıkaraoğlu, N. G. Paterakis, Y. Eren, and J. P. Catalão, "End-user comfort oriented day-ahead planning for responsive residential hvac demand aggregation considering weather forecasts," *IEEE Trans. on Smart Grid*, vol. 8, no. 1, pp. 362–372, 2017.

[3] Y. Lin, P. Barooah, S. Meyn, and T. Middelkoop, "Experimental evaluation of frequency regulation from commercial building hvac systems," *IEEE Trans. on Smart Grid*, vol. 6, no. 2, pp. 776–783, 2015.

[4] J. H. Yoon, R. Baldick, and A. Novoselac, "Dynamic demand response controller based on real-time retail price for residential buildings," *IEEE Trans. on Smart Grid*, vol. 5, no. 1, pp. 121–129, 2014.

[5] P. Zhao, G. Henze, S. Plamp, and V. J. Cushing, "Evaluation of commercial building hvac systems as frequency regulation providers," *Energy and Buildings*, vol. 67, pp. 225–235, Dec. 2013.

[6] E. Yao, V. Wong, and R. Schober, "A robust design of electric vehicle frequency regulation service," in *Proc. of IEEE SmartGridComm*, 2014.

[7] G. He, Q. Chen, C. Kang, P. Pinson, and Q. Xia, "Optimal bidding strategy of battery storage in power markets considering performance-based regulation and battery cycle life," *IEEE Trans. on Smart Grid*, vol. 7, no. 5, pp. 2359–2367, 2016.

[8] K. Ko, S. Han, and D. K. Sung, "Performance-based settlement of frequency regulation for electric vehicle aggregators," *IEEE Trans. on Smart Grid*, 2016.

[9] E. Yao, V. W. Wong, and R. Schober, "Robust frequency regulation capacity scheduling algorithm for electric vehicles," *IEEE Trans. on Smart Grid*, 2016.

[10] S. Li, M. Brocanelli, W. Zhang, and X. Wang, "Integrated power management of data centers and electric vehicles for energy and regulation market participation," *IEEE Trans. on Smart Grid*, vol. 5, no. 5, pp. 2283–2294, Sep. 2014.

[11] M. Motalleb, M. Thornton, E. Reihani, and R. Ghorbani, "A nascent market for contingency reserve services using demand response," *Applied Energy*, vol. 179, pp. 985–995, 2016.

[12] Y. Zhang, M. E. Raoufat, and K. Tomsovic, "Remedial action schemes and defense systems," *Smart Grid Handbook*, 2016.

[13] M. Motalleb, M. Thornton, E. Reihani, and R. Ghorbani, "Providing frequency regulation reserve services using demand response scheduling," *Energy Conversion and Management*, vol. 124, pp. 439–452, 2016.

[14] A. Sadeghi-Mobarakeh and H. Mohsenian-Rad, "Strategic selection of capacity and mileage bids in california iso performance-based regulation market," in *Proc. of IEEE PES General Meeting*, 2016.

[15] California ISO, "Business Requirements Specification - Pay For Performance Regulation," May 2013.

[16] R. N. Allan, *Reliability evaluation of power systems*. Springer Science & Business Media, 2013.

[17] M. Farajollahi, M. Fotuhi-Firuzabad, and A. Safdarian, "Deployment of fault indicator in distribution networks: A mip-based approach," *IEEE Transactions on Smart Grid*, 2016.

[18] A. Shahsavari, S. M. Mazhari, A. Fereidunian, and H. Lesani, "Fault indicator deployment in distribution systems considering available control and protection devices: a multi-objective formulation approach," *IEEE Trans. on Power System*, vol. 29, no. 5, pp. 2359–2369.

[19] T. A. Short, *Distribution reliability and power quality*. CRC Press, 2005.

[20] A. Sadeghi-Mobarakeh and H. Mohsenian-Rad, "Optimal bidding in performance-based regulation markets: An mpec analysis with system dynamics," *IEEE Trans. on Power Systems*, vol. 32, no. 2, pp. 1282–1292, 2017.

[21] PJM. [Online]. Available: https://www.pjm.com/ /media/committees-groups/subcommittees/drs/20150224/20150224-item-03b-draft-manual-12-version-32-regulation-redlines.ashx

[22] E. Mallada, C. Zhao, and S. Low, "Optimal load-side control for frequency regulation in smart grids," in *Proc. of Allerton Communication, Control, and Computing*, 2014.

[23] [Online]. Available: http://pqubepmu.com

[24] J. H. Eto, E. Stewart, T. Smith, M. Buckner, H. Kirkham, F. Tuffner, and D. Schoenwald, "Scoping study on research and development priorities for distribution-system phasor measurement units," 2015.

[25] C. Shand, A. McMorran, E. Stewart, and G. Taylor, "Exploiting massive pmu data analysis for lv distribution network model validation," in *Proc. of IEEE Power Engineering Conference (UPEC)*, 2015.

[26] A. Shahsavari, M. Farajollahi, E. Stewart, A. von Meier, L. Alvarez, E. Cortez, and H. Mohsenian-Rad, "A data-driven analysis of capacitor bank operation at a distribution feeder using micro-pmu data," in *Proc. of IEEE PES Innovative Smart Grid Technologies Conference*, Washington D.C., Apr. 2017.

[27] A. Shahsavari, A. Sadeghi-Mobarakeh, E. Stewart, and H. Mohsenian-Rad, "Distribution grid reliability analysis considering regulation down load resources via micro-pmu data," in *Proc. of IEEE International Conference on Smart Grid Communications*, Sydney, Australia, Nov. 2016.

[28] M. Farajollahi, A. Shahsavari, and H. Mohsenian-Rad, "Location identification of high impedance faults using synchronized harmonic phasors," in *Proc. of IEEE PES Innovative Smart Grid Technologies Conference*, Washington D.C., Apr. 2017.

[29] J. Bezdek, R. Ehrlich, and W. Full, "FCM: The fuzzy c-means clustering algorithm," *Computers & Geosciences*, vol. 10, no. 2, pp. 191–203, 1984.

[30] W. Kersting, *Distribution system modeling and analysis*. CRC, 2012.

[31] A. Pradhan, A. Routray, and S. M. Gudipalli, "Fault direction estimation in radial distribution system using phase change in sequence current," *IEEE Trans. on Power System*, vol. 22, no. 4, pp. 2065–2071, Oct. 2007.

[32] T. E. Mcdermott and G. Benmouyal, "Ieee standard inverse-time characteristic equations for overcurrent relays. discussion," *IEEE Trans. on Power Delivery*, vol. 14, no. 3, pp. 868–872.

[33] AREVA. [Online]. Available: http://mt.schneider-electric.be/op_main/micom/p12x_en_da6.pdf

[34] D. Li and L. Qi, "Energy based fuse modeling and simulation," in *Proc. of IEEE Electric Ship Technologies Symposium (ESTS)*, 2013.

[35] B. Hegde, S. Midlam-Mohler, and P. J. Tulpule, "Thermal model of fuse dynamics for simulation under intermittent dc faults," in *Proc. of ASME Dynamic Systems and Control*, 2015.

[36] T. A. Short, *Electric power distribution handbook*. CRC press, 2014.

[37] Eaton, "Medium Voltage Expulsion Fuses," May 2002.

[38] R. N. Allan, R. Billinton, I. Sjarief, L. Goel, and K. So, "A reliability test system for educational purposes-basic distribution system data and results," *IEEE Trans. on Power System*, vol. 6, no. 2, pp. 813–820, May 1991.

[39] M. E. Raoufat, A. Taalimi, K. Tomsovic, and R. Hay, "Event analysis of pulse-reclosers in distribution systems through sparse representation," *Proc. of International Conference on Intelligent System Application to Power Systems*, Sep. 2017.

[40] S. Chaitusaney and A. Yokoyama, "Prevention of reliability degradation from recloser–fuse miscoordination due to distributed generation," *IEEE Trans. on Power Delivery*, vol. 23, no. 4, pp. 2545–2554, 2008.

[41] S. M. Brahma and A. A. Girgis, "Microprocessor-based reclosing to coordinate fuse and recloser in a system with high penetration of distributed generation," in *Proc. of IEEE PES Winter Meeting*, 2002.

Alireza Shahsavari (S17) received the M.Sc. degree in electrical engineering - power systems from the University of Tehran, Tehran, Iran, in 2013. He received Best Master Thesis National Award, Iran, 2014. He is currently working toward his Ph.D. degree in electrical and computer engineering at the University of California, Riverside, CA, USA. His research interests include the data analysis in power systems and smart grid, distribution system planning and operation, and power system reliability.

Ashkan Sadeghi-Mobarakeh (S15) received the M.Sc. degree in energy systems engineering from the Sharif University of Technology, Tehran, Iran, in 2012. He is currently working toward his Ph.D. degree in electrical and computer engineering at the University of California, Riverside, CA, USA. His research interests include the application of operation research, mathematical optimization, and data mining techniques in electricity markets, power systems, and smart grid

Emma M Stewart completed her undergraduate degree in electrical and mechnical engineering from the University of Strathclyde in 2004, and a PhD in electrical engineering in 2009. She joined BEW Engineering (Now DNV GL) in 2009, and held the position of senior engineer in the Transmission and Distribution team, where she led distribution studies for interconnection and high renewable penetration studies for large utilities. Dr. Stewart joined Lawrence Berkeley National Laboratory in 2009, and was the deputy group leader for grid integration. Dr. Stewart recently joined the Global Security team at Lawrence Livermore National Laboratory, and is the Deputy Associate Program Leader for Infrastructure Systems.

Ed Cortez is Principal Electrical Engineer at Riverside Public Utilities. He is responsible for managing a staff of over 25 employees in the Communications, System Planning, Substation Engineering and Protection groups. He directs and supervises the deployment and integration of electric systems to support the business processes related with advanced grid technologies and system reliability. He is also responsible for the development and implementation of goals, objectives, policies and priorities of the electric utility..

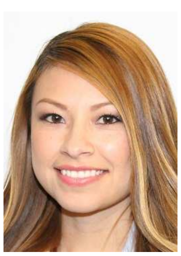

Lilliana Alvarez earned her Bachelors Degree in Electrical Engineering from California State Polytechnic University, Pomona in 2012. She began her career at Riverside Public Utilities as an intern in August 2012 and was promoted to Utilities Associate Electrical Engineer in 2013. Lilliana now holds the position of Utilities Electrical Engineer within the Electric System Planning Department. Lillianas experience includes transmission and distribution planning, project management, underground cable modeling, and power quality.

PLACE PHOTO HERE

Fady Megala is a Utilities Senior Electrical Engineer within the Substations Department at Riverside Public Utilities.

Hamed Mohsenian-Rad (S04M09SM14) received the Ph.D. degree in electrical and computer engineering from the University of British Columbia Vancouver, BC, Canada, in 2008. He is currently an Associate Professor of electrical engineering at the University of California, Riverside, CA, USA. His research interests include modeling, data analysis, and optimization of power systems and smart grids. He received the National Science Foundation CAREER Award 2012, the Best Paper Award from the IEEE Power and Energy Society General Meeting 2013, and the Best Paper Award from the IEEE International Conference on Smart Grid Communications 2012. He serves as an Editor for the IEEE TRANSACTIONS ON SMART GRID and the IEEE POWER ENGINEERING LETTERS.